



Copyright Infopro Digital Limited 2022. All rights reserved. You may share using our article tools. This article may be printed for the sole use of the Authorised User (named subscriber), as outlined in our terms and conditions. <https://www.infopro-insight.com/termsconditions/insight-subscriptions>

Research Paper

A multivariate model for hybrid wind–photovoltaic power production with energy portfolio optimization

Laura Casula,¹ Guglielmo D’Amico,² Giovanni Masala¹ and Filippo Petroni³

¹Dipartimento di Scienze Economiche e Aziendali, Università degli Studi di Cagliari, 09123 Cagliari, Italy; emails: laura.casula@gmail.com, gb.masala@unica.it

²Dipartimento di Economia, Università degli Studi “G. D’Annunzio” Chieti–Pescara, 66013 Chieti, Italy; email: g.damico@unich.it

³Dipartimento di Management, Università Politecnica delle Marche, 60121 Ancona, Italy; email: f.petroni@univpm.it

(Received November 1, 2021; revised June 9, 2022; accepted June 30, 2022)

ABSTRACT

Generation of renewable energy is destined to grow further, motivated, for example, by the Paris Agreement, aimed at reducing the production of greenhouse gases. In particular, hybrid production plants allow the exploitation of different climatic sources to generate electricity. We analyze the electricity generation of a mixed wind–photovoltaic (PV) system, considering a multivariate model that involves the required climatic variables. We include the price of electricity in our model in order to evaluate the profitability of the system through its expected income. In addition, we investigate the optimal choice between these two production technologies via Markowitz’s classic portfolio selection theory. To this end, we then consider a portfolio of the income deriving from both wind and PV production. We determine the most efficient components that maximize the overall income of our portfolio. This analysis is enriched by taking into consideration the loss of load hours of efficient

portfolios. Finally, we make an optimal choice between the two technologies. The models are validated via Monte Carlo simulations using empirical data.

Keywords: renewable energy; income; Monte Carlo simulation; electricity price; efficient frontier; loss of load hours (LoLH).

1 INTRODUCTION

The production of renewable energy is destined to continue its expansion in the coming years because it is characterized by, among other things, its reduced environmental impact. In fact, wind and photovoltaic (PV) power, for example, make it possible to exploit climatic variables such as wind speed and solar radiation. Renewable energy also has an important impact on the formulation of electricity prices within the auction mechanism that characterizes the day-ahead electricity market.

The importance of renewable energy is also highlighted in the 2015 Paris Agreement, settled by the United Nations Framework Convention on Climate Change (see Framework Convention on Climate Change 2015, Section 7d), which aims to mitigate climate change by reducing greenhouse gas emissions and thus their “greenhouse effect”.

Various aspects of the development of renewable energies have been addressed in the specialized literature. For example, Patlitzianas and Flamos (2016) analyze renewable energy development in the Gulf Cooperation Council countries; Pekez *et al* (2016) show how the expansion of renewable energy sources (RES) is a possible solution to the emissions associated with climate change. In addition, Das and Malakar (2021) deal with the uncertainty in the production of wind farms with particular regard to the profit margin in the Indian energy market. Hybrid systems using wind generators and PV panels are increasingly used (see, for example, Ferrer-Martí *et al* 2013; Domenech *et al* 2019). These systems are very complex and involve different technologies for energy production.

The themes we develop in this work are detailed below.

- (1) We aim to model the overall energy production of a hybrid wind–photovoltaic system in a given location. Suppose we know the technical characteristics and the nominal value of the wind turbine and the photovoltaic panel. To this end, we should model the main stochastic climatic variables involved in this process: solar radiation, wind speed and temperature.
- (2) After estimating the overall energy produced in a given period, we determine the expected income in that period by including the electricity price. We must therefore model the zonal electricity price linked to the chosen location.

- (3) Finally, we focus on the optimal choice between the two production technologies. To do this, we use the classic Markowitz portfolio selection theory (Markowitz 1952). We consider a portfolio consisting of the expected income from both wind and PV production and determine the optimal mix that maximizes the total income of our portfolio. In addition, we consider another typical risk indicator of energy production: the loss of load hours (LoLH), which gives the total number of hours for a given horizon for which the production of energy is lower than that planned. Once we have determined the set of efficient portfolios using financial techniques based on Markowitz theory, we select the most efficient portfolio, which has the desired value for the LoLH indicator.

Below we examine how these aspects have been addressed in the recent, specialized literature as well as their limitations, which we intend to address.

1.1 Climatic variables

The literature on temperature modeling includes Benth and Benth (2011), Huang *et al* (2018), Lee and Craine (2012), Türkvtan *et al* (2020) and Zapranis and Alexandridis (2011). These surveys highlight the main characteristics of the temperature (eg, seasonality and autoregressive features).

Regarding wind speed, we refer the reader to the following contributions to the literature. Caporin and Preš (2012) show that the autoregressive fractionally integrated moving average–fractionally integrated generalized autoregressive conditionally heteroscedastic (ARFIMA-FIGARCH) process models wind speed efficiently. Chang (2011) applies the Weibull distribution (which fits the typical distribution shapes of the wind speed characteristics), with parameters estimated with the maximum likelihood estimation method. D’Amico *et al* (2015a) simulate wind speed through indexed semi-Markov chains. Sim *et al* (2019) initially apply a particular distribution to the data and then apply autoregressive integrated moving average processes.

Solar radiation was studied by Saoud *et al* (2018) through a quaternion-valued neural network for short-term forecasting purposes. Some works use neural network techniques to determine PV energy production (see, for example, Monteiro *et al* 2017; Yousif *et al* 2017; Graditi *et al* 2016). Benth and Ibrahim (2017) apply a continuous-time process, and Lingohr and Müller (2019) apply a nonlinear continuous-time autoregressive process to model PV production. The efficiency of a PV panel has been studied by several authors. For the determination of the modular temperature of a PV panel, we follow Faiman’s law (Faiman 2008). To establish the technical characteristics of the PV panel in our study, we refer to Huld *et al* (2011), Koehl *et al* (2011) and Urraca *et al* (2018). The impact of temperature on PV panels’ production was examined by Dubey *et al* (2013), Singh and Ravindra (2012)

and Barykina and Hammer (2017). For this reason, we should include temperature among the stochastic variables to be modeled. However, we observe that the impact of temperature on PV production is small, so we will only consider its deterministic component.

For PV energy, for a fixed set of defined technical characteristics (size, semiconductor material, inclination, azimuth angle, etc), a panel's efficiency depends on the incident solar radiation and, to a certain extent, on other climatic variables such as wind intensity and temperature, while wind energy mainly depends on the intensity of the wind, and the energy produced can be quantified through the power curve that characterizes the turbine.

A hybrid plant makes it possible to exploit very different situations: during the night the plant will be able to produce only wind energy, while in the daytime there will be mixed production, dependent on the meteorological conditions.

The models we use for the individual climatic variables do not differ from those highlighted in the literature concerning their specific characteristics. We refer the reader to the relevant sections for more details. The innovative aspect of this paper is that we model the aforementioned variables using a multivariate model that can take into account the complex dependence structure between these variables. In this regard, we use a vector autoregressive (VAR) model. Our aim is to show that, with this approach, the total energy production from a mixed wind–photovoltaic plant can be faithfully reproduced, while the same level of production obtained by modeling the climatic variables independently yields a distorted result.

1.2 Electricity price modeling

A considerable amount of literature has been produced on the modeling of electricity prices. Fundamental references are Weron (2014) and Nowotarski and Weron (2018) (see also the references therein). In a recent contribution, Giordano and Morale (2021) apply a fractional Brownian–Hawkes model to the Italian electricity market.

The income from renewable energy sources is scarcely studied in the literature. An application to wind farms was carried out by Benth *et al* (2018), who applied an Ornstein–Uhlenbeck process to model wind speed and energy production and a normal inverse Gaussian process to represent the electricity log prices. One of the aims of our paper is to model effectively the dependence between wind speed and the price of electricity. Another application in the same sector was studied by Casula *et al* (2020a), who apply a multivariate VAR process to jointly represent the wind speed and electricity price. From this point of view, the link between climatic variables and power price is highly relevant. For example, Matsumoto and Endo (2021) aimed to forecast the price of electricity based on the forecast of climatic variables.

To effectively model the income of a hybrid plant, we extend the approach described in the abovementioned references and consider a multivariate model in which we include (in addition to the climatic variables) the price of electricity via a VAR model. This feature again represents the innovative aspect of our proposal. In this way, we can take into account the complex dependence structure between the price of electricity and climatic variables. A note of caution, however, is that the income on a given horizon is correctly represented by our model, but if we model the individual stochastic variables independently, we obtain a significantly worse result.

1.3 Portfolio selection techniques

Portfolio selection techniques in the energy sector have been addressed by several authors. Cucchiella *et al* (2017) carry out an economic analysis to evaluate the profitability of investments in RES in the Italian market, in terms of incentives. Cunha and Ferreira (2014) apply the classical mean–variance approach to a portfolio of RES (ie, hydroelectric, wind and PV) in the Portuguese market. deLlano-Paz *et al* (2017) review the literature on applications of portfolio theory to energy planning and electricity production. They state that the inclusion of RES reduces portfolio risk. Muñoz *et al* (2009) consider a portfolio consisting of wind, PV, mini-hydro and thermoelectric sources in the Spanish market. The associated cashflows are used to set the internal rate of return, and consequently to minimize the investment risk (and maximize the return) of the portfolio. Neto *et al* (2017) apply portfolio theory for hydroelectric, wind and PV assets for the Brazilian market and perform an economic analysis considering taxation and financing. Further, the need to consider energy portfolios in terms of mixtures of available generation technologies is extensively investigated by Lucheroni and Mari (2017, 2018) concerning minimization strategies for the levelized cost of energy of the portfolio. Li *et al* (2017) investigate the impact of wind and PV production on development in China. Yang *et al* (2016) examine the consumer preference for electricity generation when the share of RES increases. Mahesh and Sandhu (2015) examine the advantages of considering hybrid wind–PV energy systems due to their complementary characteristics. From a more specific point of view, Carpio (2021) tackles the problem of intermittency in the production of PV energy through an optimal portfolio selection with a survey conducted in Brazil.

1.4 Our model, and the structure of the paper

The innovative aspects of our paper regarding portfolio selection are that we use a multivariate model to link climate variables with the price of electricity, we consider an additional risk measure that is more specific to the energy field (namely LoLH) and we highlight how LoLH can be effectively estimated using the proposed model.

We carry out a Monte Carlo simulation of the stochastic variables needed to implement the models and consider a hypothetical energy plant in Italy. (The data on solar radiation and climatic variables come from NASA's MERRA-2 project, and the data containing historical values of electricity prices come from Gestore Mercati Elettrici (GME).)

The remainder of the paper is structured as follows. In Section 2 we describe the production of wind and PV energy as well as the auxiliary variables. Section 3 discusses the modeling of the stochastic variables and we introduce the expected income. Then, in Section 4, we illustrate the results of the proposed models using the efficient frontier and LoLH estimation. Finally, Section 5 states our conclusions.

2 MATERIALS AND METHODS

In this section we first present some statistics for the variables involved in our analysis. Then, we estimate the solar energy produced by a PV panel with given characteristics and the wind energy produced by a given wind turbine.

2.1 Data set characteristics

The (hourly) time series of the climatic variables were retrieved from NASA's MERRA-2 project.¹ The geographical location chosen (39.5°N,8.75°E) is in central Sardinia, Italy, an area that is undergoing development in the field of wind farms. Obviously, as our main purpose is to obtain real-world data, the location is not very relevant for the proposed modeling.

Solar radiation is listed on MERRA-2 as the surface incoming shortwave flux (SWGDN) variable. The data set contains 40 complete years (from January 1, 1980 to December 31, 2019, on an hourly basis) and some statistics are given in Table 1.

We note that the values of solar radiation have an obvious minimum of zero (between sunset and sunrise), while the maximum value is linked to the location and the hour and day. We determine the maximum potential value (for each hour and each day of the year) empirically from the available data (this value is reached under clear-sky conditions). The actual radiation turns out to be a proportion of the maximum. Figure 1 shows the maximum radiation.

We represent the effective stochastic radiation $R(t)$ as a fraction $K(t)$ of the maximum radiation $R_{\max}(t)$ depending on the atmospheric situation. Then, for each hour of the year, we set:

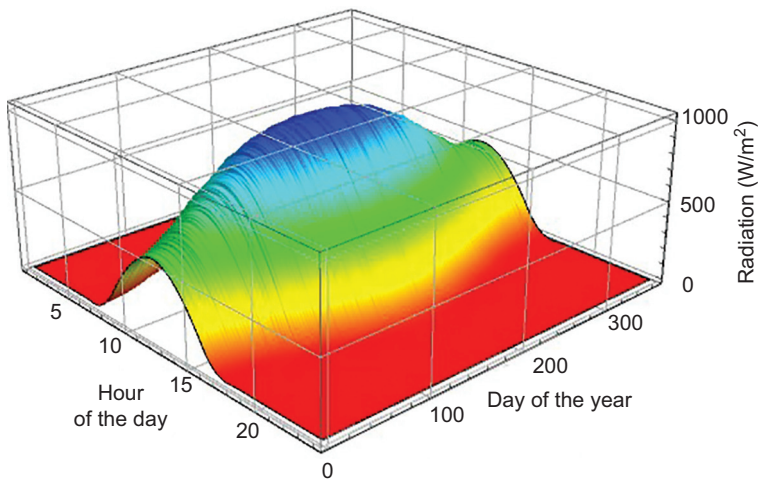
$$K(t) = \frac{R_{\max}(t) - R(t)}{R_{\max}(t)} \in [0, 1], \quad t = 1, \dots, 8760. \quad (2.1)$$

¹ URL: <https://gmao.gsfc.nasa.gov/reanalysis/MERRA-2>.

TABLE 1 Solar radiation, temperature, wind speed and electricity price: real values.

	Solar radiation (W/m ²)	Temperature (°C)	Wind speed (m/s)	Electricity price (€/MWh)
Mean	205.96	17.52	6.54	63.88
Standard deviation	287.70	9.75	3.51	34.19
Skewness	1.22	0.65	0.78	2.49
Kurtosis	3.19	2.96	3.62	12.38
Minimum	0.00	-3.63	0.02	0.00
Maximum	1 030.00	49.68	26.08	450.00
Observations	350 640	78 888	78 888	78 888

FIGURE 1 Maximum radiation versus day and hour.



Equation (2.1) holds when $R_{\max}(t) \neq 0$; otherwise the radiation is zero.

As a consequence, $R(t) = R_{\max}(t)(1 - K(t))$. This process has a seasonal component (periods of one year and 24 hours) and an autoregressive component with two lags. These features are deduced by analyzing the periodogram and the autocorrelation function (ACF) and partial autocorrelation function (PACF) (Casula *et al* 2020b).

The temperature is given by the TS variable in the MERRA-2 data set. The data ranges from January 1, 2009 to December 31, 2017 (some statistics are illustrated in

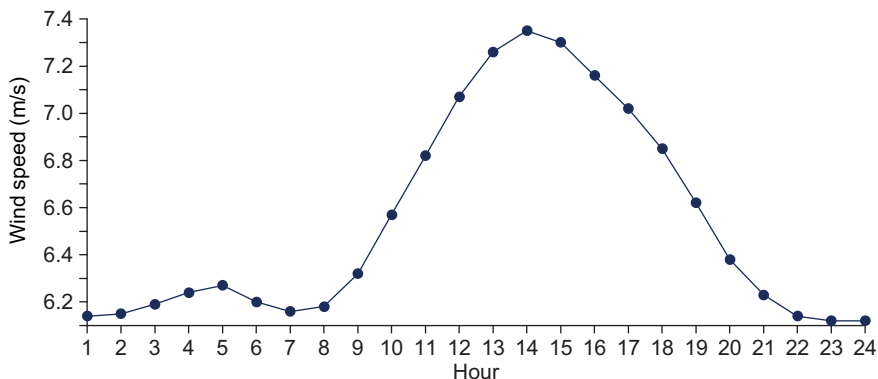
FIGURE 2 Mean wind speed versus hour of the day.

Table 1). The series has a well-known seasonal trend. The seasonal component has two main periods (one year, and 24 hours) and the autoregressive component is an AR(3) process. The optimal lag is determined with the Akaike information criterion (AIC) and the Bayesian information criterion (BIC).

The wind speed components are given in the MERRA-2 data set as the variables two-meter eastward wind (U2M) and two-meter northward wind (V2M). The data ranges from January 1, 2009 to December 31, 2017 (some statistics are given in Table 1).

We deduce from Figure 2 that the mean wind speed is linked to the hour of the day. The average speed peaks at about 14:00.

Finally, we deduce from the inspection of the ACF and PACF that lags 1 and 2 are significant, and additionally that the series shows a seasonality of 24 hours and one year (Casula *et al* 2020a).

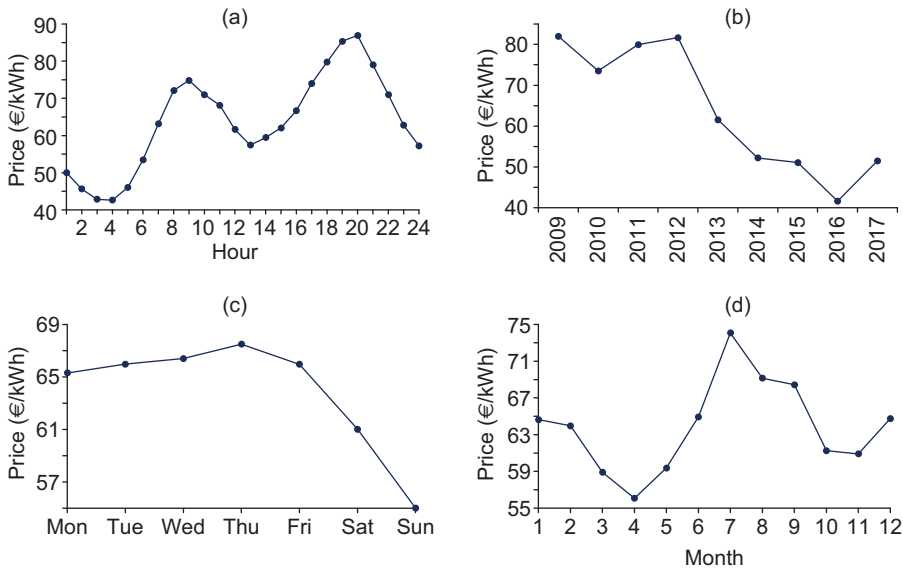
The electricity price data set ranges from January 1, 2009 to December 31, 2017 and is available from the Gestore Mercati Energetici website.² We used the Sardinia zonal price (some statistics are illustrated in Table 1). We deduce a high value of kurtosis caused by the numerous price peaks.

The hourly dependence of the price is shown in Figure 3(a). For example, the highest values are reached at 10:00 and 20:00 and the lowest ones at night (indeed, energy demand decreases overnight).

We observe (Figure 3(b)) that the mean price depends on the year (highest value occurred in 2009, and the lowest in 2016). The price trend is compared with the day of the week in Figure 3(c). We highlight that the average price is lower on Saturday

² URL: www.mercatoelettrico.org/It/download/DatiStorici.aspx.

FIGURE 3 Mean electricity price versus (a) hour (b) year, (c) day of the week and (d) month.



and Sunday, while on the other days lower average fluctuations occur. The dependence on the month is shown in Figure 3(d). The seasonal component contains three main periods (one year, one week and 24 hours) and the autoregressive component, deduced from the inspection of the ACF and the PACF, has two significant lags (see Casula *et al* 2020a).

2.2 Photovoltaic energy production

In this section we aim to estimate the PV energy production for a solar panel with known characteristics, given the necessary climatic factors. To this end, we follow a procedure developed by Urraca *et al* (2018). The “standard test conditions” (STC) apply with a temperature of 25 °C and an irradiation value of 1000 W/m². The electricity generated by a PV panel is a function of the in-plane radiation G_{eff} and the module temperature T_{mod} determined by the Faiman relation (Faiman 2008):

$$T_{\text{mod}} = T_{\text{amb}} + \frac{G_{\text{eff}}}{u_0 + u_1 WS_{\text{mod}}}, \quad (2.2)$$

where u_0 and u_1 are two parameters representing the effect of the radiation on the module temperature and the cooling by the wind, respectively, T_{amb} is the ambi-

TABLE 2 Turbine characteristics.

Hub height	95 m
Rated power	2 MW
Cut-in wind speed	4 m/s
Rated wind speed	13 m/s
Cut-out wind speed	25 m/s

ent temperature and WS_{mod} is the wind speed. The solar energy produced, P_{DC} , in general conditions is given by (Urraca *et al* 2018)

$$P'_{\text{DC}} = G'_{\text{eff}}(1 + k_1 \ln G'_{\text{eff}} + k_2 \ln^2 G'_{\text{eff}} + k_3 T'_{\text{mod}} + k_4 T'_{\text{mod}} \ln G'_{\text{eff}} + k_5 T'_{\text{mod}} \ln^2 G'_{\text{eff}} + k_6 T'^2_{\text{mod}}) \quad (2.3)$$

with

$$P'_{\text{DC}} = \frac{P_{\text{DC}}}{P_{\text{STC}}}, \quad G'_{\text{eff}} = \frac{G_{\text{eff}}}{G_{\text{STC}}}, \quad T'_{\text{mod}} = T_{\text{mod}} - T_{\text{STC}},$$

where P_{STC} denotes the nominal power, $G_{\text{STC}} = 1000 \text{ W/m}^2$ and $T_{\text{STC}} = 25 \text{ }^\circ\text{C}$. The parameters k_1, \dots, k_6 characterize the type of panels.

2.3 Wind energy production

We consider a turbine with the characteristics shown in Table 2 (see Casula *et al* 2020a).

The wind speed is then transformed into wind power through the power curve $\Psi(x)$, which characterizes the turbine:

$$\Psi(x) = \begin{cases} 0 & \text{if } 0 < x < 4, \\ 21.78x^2 - 147.96x + 243.42 & \text{if } 4 \leq x \leq 13, \\ 2000 & \text{if } 13 < x \leq 25, \\ 0 & \text{if } x > 25, \end{cases} \quad (2.4)$$

with x expressed in m/s and $\Psi(x)$ expressed in kWh. We note that the technical characteristics of a wind turbine (cut-in and cut-out wind speed, rated power, height, power curve) can be changed at will without this affecting the mathematical models used. We have chosen a turbine with given characteristics simply to test the model. The power curve equation was obtained with a best-fitting analysis on empirical data (although in general, the power curve is represented by a third-degree polynomial function, following Betz's law).

The significantly variable wind energy is linked to the wind speed fluctuations (see Table 1).

Finally, note that to determine the energy produced by our hypothetical wind turbine we will have to consider the wind speed at the required height. In this regard, we can use the following formula (see, for example, D'Amico *et al* 2015b):

$$v_h = v_{h_0} \left(\frac{h}{h_0} \right)^\vartheta \quad \text{with } \vartheta = \left(\ln \frac{h}{z_0} \right)^{-1}, \quad (2.5)$$

where v_h denotes the wind speed measured at the height h of the wind turbine hub, v_{h_0} is the known value of the wind speed at the specified height h_0 ($h_0 = 2$ m) and z_0 is a parameter linked to the morphology of the site.

3 MATHEMATICAL MODELS

3.1 Univariate processes

This section is dedicated to the stochastic modeling of the main variables involved in this study, which take into account the characteristics illustrated in Section 2.1. Specifically, we focus on an autoregressive description of a transformation of the solar radiation process and of the temperature process, a Box–Cox transformation of the wind speed process and the N -probability integral transform (N -PIT) transformation of the electricity price process. Finally, the autoregressive component of each variable has been replaced with a unique VAR process that considers the simultaneous evolution of the variables involved in the system. We leave out from the multivariate model only the temperature, for which we will take only the deterministic component.

The stochastic process $K(t)$ is modeled as

$$K(t) = c_1 + A_1 \sin \left(\frac{2\pi}{24}t + B_1 \right) + A_2 \sin \left(\frac{2\pi}{8760}t + B_2 \right) + \sum_{i=1}^2 \alpha_i K(t-i) + \varepsilon_1, \quad (3.1)$$

with white noise ε_1 .

We define the temperature series as

$$T(t) = c_2 + C_1 \sin \left(\frac{2\pi}{24}t + D_1 \right) + C_2 \sin \left(\frac{2\pi}{8760}t + D_2 \right) + \sum_{i=1}^3 \beta_i T(t-i) + \varepsilon_2, \quad (3.2)$$

TABLE 3 Solar radiation, temperature and wind speed: simulated series.

Indicator	Solar radiation (W/m ²)	Temperature (°C)	Wind speed (m/s)
Mean	210.03	17.43	2.81
Standard deviation	279.25	9.69	1.78
Skewness	1.09	0.00	0.99
Kurtosis	2.89	2.42	4.24
Minimum	0.00	-13.13	0.01
Maximum	999.10	47.95	12.47
Observations	350 640	140 256	140 256

TABLE 4 Parameters of the autoregressive moving average component.

	Value	p-value
AR(1)	1.7927	0.0000
AR(2)	-1.0739	0.0000
AR(3)	0.2053	0.0000

with white noise ε_2 . The parameters of the AR(3) process are given in Table 4.

Temperature is involved in Faïman's formula (see (2.2)). We note that the impact of temperature in PV power generation given by (2.2) is relatively marginal. In fact, if we only consider its deterministic component, then the energy produced and its variability vary in a range below 1%. For this reason, we only consider the deterministic component of the temperature, while for the other three variables (wind intensity, solar radiation, electricity price) we will build a multivariate stochastic model.

We denote by $W(t)$ the wind speed process (hourly basis) and perform the Box-Cox transformation,

$$f_{\xi}(x) = \frac{x^{\xi} - 1}{\xi}, \quad (3.3)$$

with the aim of making the distribution more similar to the normal distribution (see Sim *et al* 2019; Casula *et al* 2020a). We define the transformed variable as $\hat{W}(t) = f_{\xi}(W(t))$. The process $\hat{W}(t)$ is modeled as

$$\begin{aligned} \hat{W}(t) = & c_3 + E_1 \sin\left(\frac{2\pi}{24}t + F_1\right) + E_2 \sin\left(\frac{2\pi}{8760}t + F_2\right) \\ & + \sum_{i=1}^2 \delta_i \hat{W}(t-i) + \varepsilon_3, \end{aligned} \quad (3.4)$$

TABLE 5 Yearly values of the parameter ξ .

Year	ξ
2009	0.5082
2010	0.5136
2011	0.4720
2012	0.4359
2013	0.4350
2014	0.5377
2015	0.4267
2016	0.5372
2017	0.4078
2018	0.4819

with white noise ε_3 .

We then apply the inverse Box–Cox transformation,

$$f_{\xi}^{-1}(x) = (1 + \xi x)^{1/\xi}, \tag{3.5}$$

to restore the starting variable. The yearly values of the parameter ξ are shown in Table 5.

The statistics of the simulated climatic series (solar radiation, wind speed and temperature) given in Table 3 are very close to the empirical data presented in Table 1.

Finally, let $P(t)$ be the electricity price process (hourly basis) and apply to it the N -PIT transformation with the aim of making the distribution more similar to the normal distribution (Nowotarski and Weron 2018; Uniejewski *et al* 2019; Casula *et al* 2020a,b):

$$\tilde{P}(t) = G^{-1}(F_{P(t)}(P(t))), \tag{3.6}$$

where $F_{P(t)}$ is the cumulative distribution function (CDF) of $P(t)$ and G^{-1} is the inverse of the standard normal CDF. The new process $\tilde{P}(t)$ is closer to the normal distribution and its equation is

$$\begin{aligned} \tilde{P}(t) = & c_4 + M_1 \sin\left(\frac{2\pi}{24}t + N_1\right) + M_2 \sin\left(\frac{2\pi}{168}t + N_2\right) \\ & + M_3 \sin\left(\frac{2\pi}{8760}t + N_3\right) + \sum_{i=1}^2 \gamma_i \tilde{P}(t - i) + \varepsilon_4, \end{aligned} \tag{3.7}$$

with white noise ε_4 . This process has a seasonal component (periods of one day, one week and one year) and an autoregressive component with two lags. These features

TABLE 6 Simulated and real electricity price statistics for 2017.

Indicator	Real	Simulated
Mean	51.80	51.96
Standard deviation	13.37	13.11
Skewness	−0.46	−0.41
Kurtosis	4.83	4.69
Minimum	0.00	0.00
Maximum	113.07	109.57

are again deduced by analyzing the periodogram and the ACF and PACF (Casula *et al* 2020b).

Next, we just have to perform the inverse N -PIT transformation

$$P(t) = F_P^{-1}(G(\tilde{P}(t))).$$

We omit the parameters' values for the sake of brevity. The statistics of the simulated series are shown in Table 6, and they reveal an excellent fit with real data. We observe that, to determine a simulated trajectory from (3.7), for each time t in the chosen time horizon, a random number is extracted from the white noise ε_4 .

3.2 The multivariate process

The electricity price, wind speed and solar radiation are the main stochastic variables involved in this study. In the multivariate model, we modeled the variables annually, as correlations vary greatly (as can be seen from Table 7). Consequently, in the deterministic component of each variable, we have omitted the annual seasonality (periodicity of 8760 hours), as can be seen from (3.9).

From the analysis of the data, we note that the correlations between these variables vary considerably. We show in Figure 4 the correlations using a one-year rolling window for the period 2009–2018 (this means that the year-length window is rolled daily).

We notice some correlation between the price of electricity and both wind speed and solar radiation. This correlation is casual and not causal. In reality, the price of electricity is obviously linked to the demand for energy itself.

Next, we show in Table 7 the correlations for each pair of variables and each year (evaluated from actual data). These correlations change significantly from year to year. We will need to consider a multivariate model that correctly reflects this dependency structure. Single-variable processes contain a seasonal component and an autoregressive component. When moving to the multivariate model, we keep

FIGURE 4 Correlations between electricity price, wind speed and solar radiation for the years 2009–18.

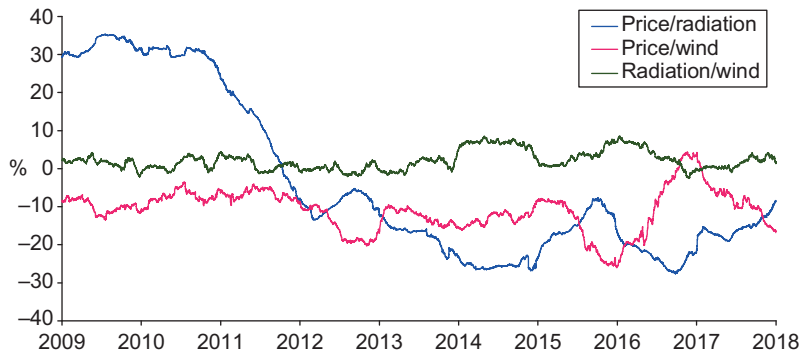


TABLE 7 Correlations between electricity price, wind speed and solar radiation for the period 2009–2017.

	Price/ radiation	Price/ wind	Radiation/ wind
2009	32.92	-11.57	2.28
2010	29.32	-6.58	0.17
2011	14.37	-4.22	1.50
2012	-9.64	-14.42	0.44
2013	-16.54	-11.28	1.16
2014	-26.14	-11.61	7.13
2015	-15.80	-11.21	3.28
2016	-22.47	-13.38	3.98
2017	-18.73	-6.69	-0.20

All values are given in percent.

the seasonal component and replace the individual autoregressive processes with a unique VAR process.

More specifically, we use a VAR(3, 2) process (with three variables and two lags).

We therefore propose the following model:

$$\left. \begin{aligned} \hat{K}(t) &= \sum_{i=1}^2 a_i \hat{K}(t-i) + \sum_{i=1}^2 b_i \hat{P}(t-i) + \sum_{i=1}^2 g_i \hat{W}(t-i) + \eta_1, \\ \hat{P}(t) &= \sum_{i=1}^2 d_i \hat{K}(t-i) + \sum_{i=1}^2 e_i \hat{P}(t-i) + \sum_{i=1}^2 f_i \hat{W}(t-i) + \eta_2, \\ \hat{W}(t) &= \sum_{i=1}^2 m_i \hat{K}(t-i) + \sum_{i=1}^2 n_i \hat{P}(t-i) + \sum_{i=1}^2 o_i \hat{W}(t-i) + \eta_3, \end{aligned} \right\} \quad (3.8)$$

where η_1 , η_2 and η_3 are white noises with associated deseasonalized processes given by

$$\left. \begin{aligned} \hat{K}(t) &= K(t) - c_1 - A_1 \sin\left(\frac{2\pi}{24}t + B_1\right), \\ \hat{P}(t) &= \tilde{P}(t) - c_4 - M_1 \sin\left(\frac{2\pi}{24}t + N_1\right) - M_2 \sin\left(\frac{2\pi}{168}t + N_2\right), \\ \hat{W}(t) &= \tilde{W}(t) - c_3 + E_1 \sin\left(\frac{2\pi}{24}t + F_1\right). \end{aligned} \right\} \quad (3.9)$$

REMARK 3.1 Some of these relationships have no direct interpretation. For example, knowing the price gives us approximate information on the time of day and, consequently, indirect information on the intensity of the wind. For example, if the price is very low, this corresponds mainly to night hours, when even the wind has low values.

3.3 The economic study

In this section, we provide a set of tools that will be useful to assess the economic adequacy of a hybrid wind–PV plant from different perspectives. Specifically, we first present a profitability investigation based on the income process. Further, we deal with the optimal mixing of the two energy technologies (wind and PV) valued using techniques of efficient portfolio selection and the computation of the LoLH, which measures the risk of an insufficient generating capacity as compared with the power demand.

3.3.1 Energy production and income

We determine the production of photovoltaic and wind energy, and then we deduct the joint production and the overall income.

For photovoltaic energy, we apply (2.2) with the following parameter values from Koehl *et al* (2011):

$$u_0 = 26.9 \text{ W/}^\circ\text{Cm}^2, \quad u_1 = 6.20 \text{ Ws/}^\circ\text{Cm}^3.$$

Next, we apply (2.3) with parameter values (given by Huld *et al* (2011) in the case of crystalline silicon panels)

$$\begin{aligned} k_1 &= -0.017237, & k_4 &= 0.000149, \\ k_2 &= -0.040465, & k_5 &= 0.000170, \\ k_3 &= -0.004702, & k_6 &= 0.000005. \end{aligned}$$

Finally, we consider a conventional nominal power $P_{\text{STC}} = 1 \text{ kW}$.

Next, we estimate the expected profit coming from the overall production of electricity for a given horizon. To this end, we consider the electricity prices. The expected income of the PV panel and the wind turbine from an initial time $t_0 \geq 0$ up to time $t_0 + \tau$ is given by

$$V(t_0, t_0 + \tau) = \mathbb{E}_{t_0} \left[\sum_{k=1}^{\tau} P(t_0 + k)z(t_0 + k)(1 + r)^{-k} \right], \quad (3.10)$$

where r is the (constant) risk-free interest rate, $P(t_0 + k)$ is the electricity price at time $t_0 + k$, and $z(t_0 + k)$ is the energy generated at time $t_0 + k$. The energy generated is a combination of both PV and wind energy. We take the following estimator of the expected income:

$$\hat{V}(t_0, t_0 + \tau) = \frac{1}{n} \sum_{i=1}^n \sum_{k=1}^{\tau} P_i(t_0 + k)z_i(t_0 + k)(1 + r)^{-k}, \quad (3.11)$$

where $P_i(t_0 + k)$ denotes the price process at time $t_0 + k$ for the i th simulated path, $z_i(t_0 + k)$ is the energy process at time $t_0 + k$ for the i th simulated path and n is the number of paths. Note that, by virtue of the VAR model specification, the processes $P_i(t_0 + k)$ and $z_i(t_0 + k)$ are mutually dependent and $z_i(t_0 + k)$ is the summation of the (dependent) power productions due to wind and solar radiation.

3.3.2 Efficient frontier

We face the problem of the optimal choice between the two energy technologies (wind and PV energy production). Specifically, a hypothetical investor can choose between the two production technologies. Some combinations will lead to a higher income but also a higher risk, measured through volatility. The ultimate goal will be to determine the set of efficient portfolios in the classic Markowitz sense. Let us

consider a portfolio composed of weights x_1 and x_2 in the two technologies (wind and PV). The income of this portfolio is the weighted sum of the incomes of both technologies. We define the expected value and the variance of the income of the two technologies from an initial time $t_0 \geq 0$ up to time $t_0 + \tau$ as

$$\begin{aligned} \mu_1 &= \mathbb{E}_{t_0} \left[\sum_{k=1}^{\tau} (P(t_0 + k) - \chi_1) z^1(t_0 + k) (1 + r)^{-k} \right], \\ \mu_2 &= \mathbb{E}_{t_0} \left[\sum_{k=1}^{\tau} (P(t_0 + k) - \chi_2) z^2(t_0 + k) (1 + r)^{-k} \right], \\ \sigma_1^2 &= \text{Var}_{t_0} \left[\sum_{k=1}^{\tau} (P(t_0 + k) - \chi_1) z^1(t_0 + k) (1 + r)^{-k} \right], \\ \sigma_2^2 &= \text{Var}_{t_0} \left[\sum_{k=1}^{\tau} (P(t_0 + k) - \chi_2) z^2(t_0 + k) (1 + r)^{-k} \right], \end{aligned}$$

where χ_1 and χ_2 represent the production costs (z^1 is the wind energy and z^2 is the PV energy; the superscript “1” is associated with wind energy, and the superscript “2” is associated with PV energy, while subscript “P” denotes the portfolio).

In the context of Markowitz’s classic portfolio selection theory, we can consider the constrained optimization problems:

$$\left. \begin{aligned} \min_{x_1, x_2} \sigma_{\text{PTF}} &= \sqrt{x_1^2 \sigma_1^2 + x_2^2 \sigma_2^2 + 2\rho x_1 x_2 \sigma_1 \sigma_2} \\ \text{subject to} & \\ x_1 \mu_1 + x_2 \mu_2 &= \bar{\mu}, \\ x_1 + x_2 &= 1, \end{aligned} \right\} \quad (3.12)$$

and

$$\left. \begin{aligned} \max_{x_1, x_2} \mu_{\text{PTF}} &= x_1 \mu_1 + x_2 \mu_2 \\ \text{subject to} & \\ \sqrt{x_1^2 \sigma_1^2 + x_2^2 \sigma_2^2 + 2\rho x_1 x_2 \sigma_1 \sigma_2} &= \bar{\sigma}, \\ x_1 + x_2 &= 1, \end{aligned} \right\} \quad (3.13)$$

where ρ is the correlation between the expected incomes of wind and PV production. The solutions of these optimization problems will be the composition weights of the efficient portfolios. Obviously, the riskiness of the portfolios depends on the riskiness of the individual factors (given by volatility) and on the correlation between

the factors themselves. In the mean–variance plan we will therefore obtain an efficient frontier of the classic parabolic type, for which portfolios with higher expected income will clearly have a greater overall risk.

3.3.3 The loss of load hours

The risk measure LoLH is the expected number of hours, for a fixed horizon, when the energy generating capacity is lower than the demand. This risk measure is more specific in the field of electricity generation than the more classic volatility of the Markowitz environment.

The LoLH estimation involves the following steps (see D’Amico *et al* 2020).

- (1) Fix a horizon of length T .
- (2) Using the Monte Carlo procedure from the abovementioned models, simulate n trajectories of the energy produced by the plant. These trajectories can be described by the following matrix:

$$\begin{pmatrix} z_{11} & z_{12} & \cdots & z_{1T} \\ z_{21} & z_{22} & \cdots & z_{2T} \\ \vdots & \vdots & \ddots & \vdots \\ z_{n1} & z_{n2} & \cdots & z_{nT} \end{pmatrix},$$

where z_{ij} is the energy generated by the hybrid plant at the time j in the i th simulation.

We set $z_i = \{z_{i1}, \dots, z_{iT}\}$ with $i = 1, 2, \dots, n$ and note that the sequences $\{z_i\}_{i=1}^n$ are n independent realizations of the same stochastic process.

- (3) Transform the matrix (z_{ij}) via the following indicator function:

$$I_{ij} = \begin{cases} 1 & \text{if } D_j > z_{ij}, \\ 0 & \text{otherwise,} \end{cases} \tag{3.14}$$

where D_j is the energy demand at the time j .

- (4) Set $\text{LoLH}_i = \sum_{j=1}^T I_{ij}$ (ie, the number of hours when demand is not met by supply). The sequence $\{\text{LoLH}_i\}_{i=1}^n$ is a random sample of size n , as the variables LoLH_i are mutually independent and identically distributed according to step 2. We use as an estimator the sample mean:

$$\widehat{\text{LoLH}} = \frac{\sum_{i=1}^n \text{LoLH}_i}{n}. \tag{3.15}$$

TABLE 8 Correlations between simulated electricity price, wind speed and solar radiation for the period 2013–17.

	Price/ radiation	Price/ wind	Radiation/ wind
2013	-19.67	-12.16	-0.65
2014	-19.27	-10.32	-0.30
2015	-17.10	-11.36	-0.39
2016	-14.84	-15.00	-1.34
2017	-13.45	-5.27	-1.07

All values are given in percent.

4 RESULTS

In this section, we report the results of the application of the econometric models to real data in order to estimate the income process and the risk measures discussed in the previous section. Finally, we compare the real and simulated values to measure the performance of the applied models. Regarding the parameters of the VAR model in (3.8), Table A1 in the online appendix shows the results referring to 2017, from which we see that the coefficients are significant. The parameters of the multivariate model in (3.9) are listed in Table A2 in the online appendix.

4.1 Energy production

Initially, we estimated (see Table 7) the correlations between electricity price, wind speed and solar radiation for the period 2013–17. Comparison with Table 8 shows that our multivariate model faithfully reproduces the correlations between the variables.

To compare the wind and PV technologies, the values are reportioned so that both have a maximum production capacity of 1 kWh. The results are obtained annually from 2013 to 2017 and are presented in Table 9.

We find a good correspondence between real values and simulated values.

4.2 Income estimation

Table 10 shows the income (for each technology and overall production) evaluated at the beginning of each year (with $r = 0.01$). We compared the results obtained in the case when the stochastic variables (wind speed, solar radiation and electricity prices) are simulated independently. As expected, from Table 11 it can be deduced that the income simulated with the multivariate model provides, in percentage terms, values closest to the real ones. Conversely, the estimated income in the case of independence always produces worse results, in terms of both percentages and systematic excess.

TABLE 9 Simulated versus real energy production (in kW) for the period 2013–17.

	PV production		Wind production		Overall production	
	Simulated	Real	Simulated	Real	Simulated	Real
2013	0.1924	0.1881	0.2289	0.2345	0.4244	0.4226
2014	0.1955	0.1916	0.2079	0.2075	0.4034	0.3991
2015	0.1957	0.1918	0.1865	0.1903	0.3822	0.3821
2016	0.1954	0.1901	0.2095	0.2141	0.4049	0.4042
2017	0.1986	0.2003	0.1963	0.1989	0.3949	0.3991

TABLE 10 Simulated versus real income (multivariate and independent) in euros for the period 2013–17.

	PV income		Wind income		Overall income		Overall income indep.
	Simulated	Real	Simulated	Real	Simulated	Real	
2013	90 924	91 993	115 055	122 320	205 979	214 313	225 408
2014	79 114	75 395	89 866	89 989	168 980	165 384	177 839
2015	81 481	80 744	79 766	80 222	161 247	160 966	171 062
2016	66 687	63 265	72 113	73 887	138 800	137 152	144 762
2017	84 149	83 495	86 388	85 849	170 537	169 344	177 560

TABLE 11 Percentage variation in the real versus simulated income (multivariate and independent) for the period 2013–2017.

Year	Multivariate	Independent
2013	−3.89	5.18
2014	2.17	7.53
2015	0.17	6.27
2016	1.20	5.55
2017	0.70	4.85

All values are given in percent.

The mean absolute percentage error (MAPE) is 1.63% for the multivariate model and 5.88% for the independent model. We again see that the multivariate model produces a better fit.

4.3 Efficient frontier, LoLH and optimal choice

In this application, we consider $\chi_1 = 0.056$ per kWh and $\chi_2 = 0.085$ per kWh (International Renewable Energy Agency 2019).

As an example, we estimated the efficient frontier for 2017 (the last year of our data set) and this is plotted in Figure 5(a). The estimated parameters are $\mu_1 = 86\,282.8$, $\mu_2 = 84\,027.2$, $\sigma_1 = 5\,706.36$, $\sigma_2 = 1\,131.11$ and $\rho = 9.87\%$. We also examined the sensitivity of the result by changing the correlation by $\pm 10\%$. We note that with a negative shift in correlation the new efficient frontier dominates the previous one. A lower risk configuration is therefore logically obtained. As might be expected, we find that the efficient portfolios with higher expected returns will also have greater riskiness. The choice between these efficient portfolios will therefore depend on the investor's risk aversion. Of all the efficient portfolios, the "optimal" portfolio will be the one that maximizes the investor's utility function (although we do not address the problem here).

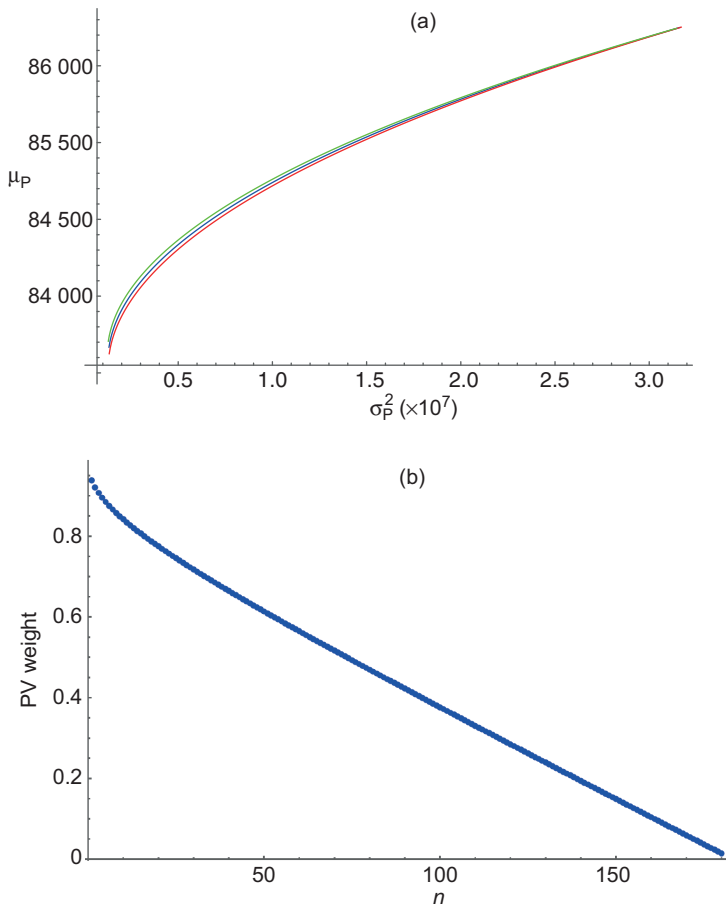
To calculate the efficient frontier, we first determined its vertex, obtained at $\sigma = 1\,125.5$. Then, we maximized the return with a fixed value of σ , starting from the minimum value obtained earlier, in increments of 25 (for a total of $n = 180$ discrete values). Finally, we imposed a constraint on the weights, included in the interval $(0, 1)$. Figure 5(b) shows the PV weights with respect to n (the number of efficient portfolios).

We note that near the vertex of the efficient frontier (the less risky portfolios) the weights are unbalanced in favor of the PV component. As we climb the efficient frontier the weights rebalance, while in the terminal part of the efficient frontier (riskier portfolios) the weights are skewed in favor of the wind component. The weights of the two components are in equilibrium when $n = 73$, corresponding to $\mu_P = 85\,150$ (the extreme values of the efficient frontier correspond to $\mu_P = 84\,166$ and $\mu_P = 86\,250$).

To perform a realistic estimate of LoLH, we calculate the real load for electricity, using data obtained from the GME website (together with electricity price data). In this way, we can consider real fluctuations in demand (so these data are not the result of a stochastic model); for example, we note that at night the energy demand is low, as is the production of energy due to climatic factors in general. The load values were then all re-proportioned to have the same order of magnitude as our hypothetical energy plant. We then compared the real and simulated LoLH for a one-year horizon (Table 12). We found good agreement between real and empirical data (the MAPE is 4.22%).

Concerning the efficient frontier determined earlier, we can calculate the value of LoLH for each efficient portfolio (in this regard see Figure 6, which represents the relationship between μ_P and LoLH values for efficient portfolios).

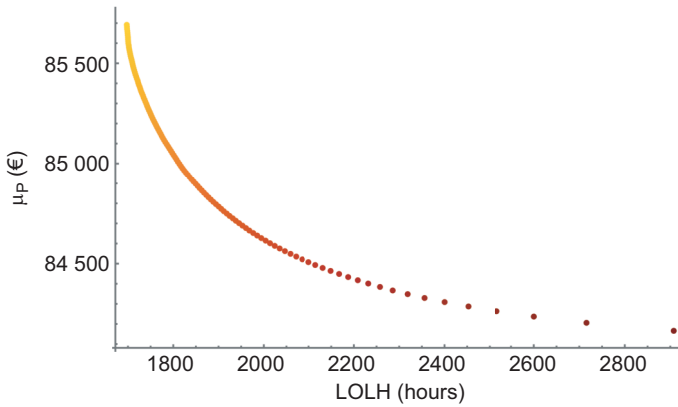
FIGURE 5 Efficient frontier for 2017 and correlation sensitivity PV weights for this efficient frontier.



(a) Upper (lower) efficient frontier with -10% ($+10\%$) correlation shift. (b) PV weights.

TABLE 12 Real versus simulated LoLH (hours) for the period 2013–17.

	Real	Simulated	Difference (%)
2013	1744	1692	3.0
2014	1648	1595	3.2
2015	1865	1780	4.6
2016	1660	1566	5.7
2017	1858	1771	4.7

FIGURE 6 Relationship between μ_P and LoLH values for efficient portfolios in 2017.

We note that the less risky efficient portfolios (with a lower expected income) have a higher LoLH. Therefore, there is a greater risk of lower energy production than required. Indeed, it is reasonable to observe that a low LoLH is associated with a high expected income: the higher the expected income, the greater the production must be, and therefore the possibility of not satisfying the demand decreases. The opposite happens for low values of the expected income.

The choice of the “optimal” portfolio should therefore stem from the comparison of these two risk measures. For example, the investor might choose the optimal portfolio as an efficient portfolio with the desired LoLH.

5 DISCUSSION

As renewable energy use is destined to increase in the future, it is necessary to develop theoretical models in order to correctly estimate the quantity of electricity produced, its economic convenience and the associated risk (understood as volumetric and market risk). This estimate obviously covers the estimate of the climatic variables involved and the zonal price of electricity. In this paper, we dealt with the generation of energy from a mixed wind–PV plant with given characteristics and in a given location. To obtain a reliable estimate of the total energy produced and the expected income, we applied a multivariate model that links the climatic variables (solar radiation and wind speed) and the electricity price, allowing us to simultaneously reproduce the dependence structure between these variables. We validated the model by verifying that the results obtained are better than modeling the individual stochastic variables independently. Further, we verified that the results obtained

through Monte Carlo simulations are significantly more reliable than those obtained from the empirical data. More precisely, first we examined the good fit of the climatic variables and the price of electricity, from which we deduced the production of wind and PV energy, and then we examined the income deriving from the production itself. For example, regarding the estimate of annual income and LoLH, the low MAPE value highlights the reasonable ability of the multivariate model to faithfully reproduce the analogous empirical values.

This multivariate model is one of the innovative elements that we have contributed to the literature.

Finally, we applied an original portfolio selection for the two technologies by considering a classic Markowitz approach (maximization of the overall expected income) and the LoLH. We observed that the use of LoLH as an additional measure of risk allows us to improve on the traditional portfolio selection method intrinsic to the classic theory of Markowitz. The goal, in fact, is to be able to choose, among all the efficient portfolios, those that meet certain requirements in terms of LoLH.

DECLARATION OF INTEREST

The authors report no conflicts of interest. The authors alone are responsible for the content and writing of the paper.

ACKNOWLEDGEMENTS

We thank the anonymous referees for their numerous constructive comments, which allowed us to significantly improve the paper.

REFERENCES

- Barykina, E., and Hammer, A. (2017). Modeling of photovoltaic module temperature using Faiman model: sensitivity analysis for different climates. *Solar Energy* **146**, 401–416 (<https://doi.org/10.1016/j.solener.2017.03.002>).
- Benth, F. E., and Benth, J. Š. (2011). Weather derivatives and stochastic modelling of temperature. *International Journal of Stochastic Analysis* **2011**, Paper 576791 (<https://doi.org/10.1155/2011/576791>).
- Benth, F. E., and Ibrahim, N. 'A., (2017). Stochastic modeling of photovoltaic power generation and electricity prices. *The Journal of Energy Markets* **10**(3), 1–33 (<https://doi.org/10.21314/JEM.2017.164>).
- Benth, F. E., Di Persio, L., and Lavagnini, S., (2018). Stochastic modeling of wind derivatives in energy markets. *Risks* **6**(2), Paper 56 (<https://doi.org/10.3390/risks6020056>).
- Caporin, M., and Preš, J. (2012). Modeling and forecasting wind speed intensity for weather risk management. *Computational Statistics and Data Analysis* **56**(11), 3459–3476 (<https://doi.org/10.1016/j.csda.2010.06.019>).

- Carpio, L. G. T. (2021). Efficient spatial allocation of solar photovoltaic electric energy generation in different regions of Brazil: a portfolio approach. *Energy Sources B* **16**(6), 542–557 (<https://doi.org/10.1080/15567249.2021.1931987>).
- Casula, L., D'Amico, G., Masala, G., and Petroni, F. (2020a). Performance estimation of a wind farm with a dependence structure between electricity price and wind speed. *World Economy* **43**(10), 2803–2822 (<https://doi.org/10.1111/twec.12962>).
- Casula, L., D'Amico, G., Masala, G., and Petroni, F. (2020b). Performance estimation of photovoltaic energy production. *Letters in Spatial and Resource Sciences* **13**, 267–285 (<https://doi.org/10.1007/s12076-020-00258-x>).
- Chang, T. P. (2011). Performance comparison of six numerical methods in estimating Weibull parameters for wind energy application. *Applied Energy* **88**(1), 272–282 (<https://doi.org/10.1016/j.apenergy.2010.06.018>).
- Cucchiella, F., Gastaldi, M., and Trosini, M. (2017). Investments and cleaner energy production: a portfolio analysis in the Italian electricity market. *Journal of Cleaner Production* **142**(1), 121–132 (<https://doi.org/10.1016/j.jclepro.2016.07.190>).
- Cunha, J., and Ferreira, P. (2014). Designing electricity generation portfolios using the mean–variance approach. *International Journal of Sustainable Energy Planning and Management* **4**, 17–30 (<https://doi.org/10.5278/ijsep.m.2014.4.3>).
- D'Amico, G., Petroni, F., and Pratico, F. (2015a). Economic performance indicators of wind energy based on wind speed stochastic modeling. *Applied Energy* **154**, 290–297 (<https://doi.org/10.1016/j.apenergy.2015.04.124>).
- D'Amico, G., Petroni, F., and Pratico, F. (2015b). Wind speed prediction for wind farm applications by extreme value theory and copulas. *Journal of Wind Engineering and Industrial Aerodynamics* **145**, 229–236 (<https://doi.org/10.1016/j.jweia.2015.06.018>).
- D'Amico, G., Masala, G., Petroni, F., and Sobolewski, R. A. (2020). Managing wind power generation via indexed semi-Markov model and copula. *Energies* **13**, Paper 4246 (<https://doi.org/10.3390/en13164246>).
- Das, P., and Malakar, T. (2021). A realistic assessment of day-ahead profit for wind farms in frequency-based energy pricing environment. *Energy Sources B* **16**(5), 443–477 (<https://doi.org/10.1080/15567249.2021.1916794>).
- deLlano-Paz, F., Calvo-Silvosa, A., Antelo, S. I., and Soares, I. (2017). Energy planning and modern portfolio theory: a review. *Renewable and Sustainable Energy Reviews* **77**, 636–651 (<https://doi.org/10.1016/j.rser.2017.04.045>).
- Domenech, B., L. Ferrer-Martí, and Pastor, R. (2019). Comparison of various approaches to design wind–PV rural electrification projects in remote areas of developing countries. *Wiley Interdisciplinary Reviews: Energy and Environment* **8**(3), Paper e332 (<https://doi.org/10.1002/wene.332>).
- Dubey, S., Sarvaiya, J. N., and Seshadri, B. (2013). Temperature dependent photovoltaic (PV) efficiency and its effect on PV production in the world: a review. *Energy Procedia* **33**, 311–321 (<https://doi.org/10.1016/j.egypro.2013.05.072>).
- Faiman, D. (2008). Assessing the outdoor operating temperature of photovoltaic modules. *Progress in Photovoltaics: Research and Applications* **16**(4), 307–315 (<https://doi.org/10.1002/pip.813>).
- Ferrer-Martí, L., Domenech, B., A. García-Villoria, and Pastor, R. (2013). A MILP model to design hybrid wind–photovoltaic isolated rural electrification projects in developing

- countries. *European Journal of Operational Research* **226**(2), 293–300 (<https://doi.org/10.1016/j.ejor.2012.11.018>).
- Giordano, L., and Morale, D. (2021). A fractional Brownian–Hawkes model for the Italian electricity spot market: estimation and forecasting. *The Journal of Energy Markets* **14**(3), 65–109 (<https://doi.org/10.21314/JEM.2021.001>).
- Graditi, G., Ferlito, S., and Adinolfi, G. (2016). Comparison of photovoltaic plant power production prediction methods using a large measured dataset. *Renewable Energy* **90**, 513–519 (<https://doi.org/10.1016/j.renene.2016.01.027>).
- Huang, W., Jr., Yang, S. S., and Chang, C.-C. (2018). Modeling temperature behaviors: application to weather derivative valuation. *Journal of Futures Markets* **38**(9), 1152–1175 (<https://doi.org/10.1002/fut.21923>).
- Huld, T., Friesen, G., Skoczek, A., Kenny, R. P., Sample, T., Field, M., and Dunlop, E. D. (2011). A power-rating model for crystalline silicon PV modules. *Solar Energy Materials and Solar Cells* **95**(12), 3359–3369 (<https://doi.org/10.1016/j.solmat.2011.07.026>).
- International Renewable Energy Agency (2019). Renewable power generation costs in 2018. Report, IRENA, Abu Dhabi. URL: www.irena.org/publications/2019/May/Renewable-power-generation-costs-in-2018.
- Koehl, M., Heck, M., Wiesmeier, S., and Wirth, J. (2011). Modeling of the nominal operating cell temperature based on outdoor weathering. *Solar Energy Materials and Solar Cells* **95**(7), 1638–1646 (<https://doi.org/10.1016/j.solmat.2011.01.020>).
- Lee, J., and Craine, R. (2012). Temperature modeling and weather derivative pricing. *American Journal of Scientific Research* **77**, 93–109. URL: <https://bit.ly/3R2l4np>.
- Li, Y., Cai, W., and Wang, C. (2017). Economic impacts of wind and solar photovoltaic power development in China. *Energy Procedia* **105**, 3440–3448 (<https://doi.org/10.1016/j.egypro.2017.03.787>).
- Lingohr, D., and Müller, G. (2019). Stochastic modeling of intraday photovoltaic power generation. *Energy Economics* **81**, 175–186 (<https://doi.org/10.1016/j.eneco.2019.03.007>).
- Lucheroni, C., and Mari, C. (2017). CO2 volatility impact on energy portfolio choice: a fully stochastic LCOE theory analysis. *Applied Energy* **190**, 278–290 (<https://doi.org/10.1016/j.apenergy.2016.12.125>).
- Lucheroni, C., and Mari, C. (2018). Risk shaping of optimal electricity portfolios in the stochastic LCOE theory. *Computers and Operations Research* **96**, 374–385 (<https://doi.org/10.1016/j.cor.2018.02.011>).
- Mahesh, A., and Sandhu, K. S. (2015). Hybrid wind/photovoltaic energy system developments: critical review and findings. *Renewable and Sustainable Energy Reviews* **52**, 1135–1147 (<https://doi.org/10.1016/j.rser.2015.08.008>).
- Markowitz, H. M. (1952). Portfolio selection. *Journal of Finance* **7**, 77–91 (<https://doi.org/10.1111/j.1540-6261.1952.tb01525.x>).
- Matsumoto, T., and Endo, M. (2021). One-week-ahead electricity price forecasting using weather forecasts, and its application to arbitrage in the forward market: an empirical study of the Japan Electric Power Exchange. *The Journal of Energy Markets* **14**(3), 39–64 (<https://doi.org/10.21314/JEM.2021.004>).
- Monteiro, R. V., Guimarães, G. C., Moura, F. A., Albertini, M. R., and Albertini, M. K. (2017). Estimating photovoltaic power generation: Performance analysis of artificial neural networks, support vector machine and Kalman filter. *Electric Power Systems Research* **143**, 643–656 (<https://doi.org/10.1016/j.epsr.2016.10.050>).

- Muñoz, J. I., de la Nieta, A. A. S., Contreras, J., and Bernal-Agustín, J. L. (2009). Optimal investment portfolio in renewable energy: the Spanish case. *Energy Policy* **37**, 5273–5284 (<https://doi.org/10.1016/j.enpol.2009.07.050>).
- Neto, D. P., Domingues, E. G., Coimbra, A. P., de Almeida, A. T., Alves, A. J., and Calixto, W. P. (2017). Portfolio optimization of renewable energy assets: hydro, wind, and photovoltaic energy in the regulated market in Brazil. *Energy Economics* **64**, 238–250 (<https://doi.org/10.1016/j.eneco.2017.03.020>).
- Nowotarski, J., and Weron, R. (2018). Recent advances in electricity price forecasting: a review of probabilistic forecasting. *Renewable and Sustainable Energy Reviews* **81**, 1548–1568 (<https://doi.org/10.1016/j.rser.2017.05.234>).
- Patlitzianas, K. D., and Flamos, A. (2016). Driving forces for renewable development in GCC countries. *Energy Sources B* **11**(3), 244–250 (<https://doi.org/10.1080/15567249.2011.616571>).
- Pekez, J., Radovanovc, L., Desnica, E., and Lambic, M. (2016). The increase of exploitability of renewable energy sources. *Energy Sources B* **11**(1), 51–57 (<https://doi.org/10.1080/15567249.2011.580318>).
- Saoud, L. S., Rahmoune, F., Tourtchine, V., and Baddari, K. (2018). A novel method to forecast 24h of global solar irradiation. *Energy Systems* **9**(1), 171–193 (<https://doi.org/10.1007/s12667-016-0218-4>).
- Sim, S.-K., Maass, P., and Lind, P. G. (2019). Wind speed modeling by nested ARIMA processes. *Energies* **12**(1), Paper 69 (<https://doi.org/10.3390/en12010069>).
- Singh, P., and Ravindra, N. M. (2012). Temperature dependence of solar cell performance: an analysis. *Solar Energy Materials and Solar Cells* **101**, 36–45 (<https://doi.org/10.1016/j.solmat.2012.02.019>).
- Türkvtan, A., Azize, H., and Omay, T. (2020). A regime switching model for temperature modeling and applications to weather derivatives pricing. *Mathematics and Financial Economics* **14**, 1–42 (<https://doi.org/10.1007/s11579-019-00242-0>).
- Uniejewski, B., Weron, R., and Ziel, F. (2019). Variance stabilizing transformations for electricity spot price forecasting. *IEEE Transactions on Power Systems* **33**(2), 2219–2229 (<https://doi.org/10.1109/TPWRS.2017.2734563>).
- United Nations Framework Convention on Climate Change (2015). Environment. In Paris Agreement, Chapter XXVII. United Nations Treaty Series, Volume 3156. UNFCCC, Bonn. URL: <https://bit.ly/3QM5sF2>.
- Urraca, R., Huld, T., Lindfors, A. V., Riihelä, A., Martinez-de-Pison, F. J., and Sanz-Garcia, A. (2018). Quantifying the amplified bias of PV system simulations due to uncertainties in solar radiation estimates. *Solar Energy* **176**, 663–677 (<https://doi.org/10.1016/j.solener.2018.10.065>).
- Weron, R. (2014). Electricity price forecasting: a review of the state-of-the-art with a look into the future. *International Journal of Forecasting* **30**, 1030–1081 (<https://doi.org/10.1016/j.ijforecast.2014.08.008>).
- Yang, Y., Solgaard, H. S., and Haider, W. (2016). Wind, hydro or mixed renewable energy source: Preference for electricity products when the share of renewable energy increases. *Energy Policy* **97**, 521–531 (<https://doi.org/10.1016/j.enpol.2016.07.030>).
- Yousif, J. H., Hussein, A. K., and Boland, J. (2017). Predictive models for photovoltaic electricity production in hot weather conditions. *Energies* **10**(7), Paper 971 (<https://doi.org/10.3390/en10070971>).

Zapranis, A. D., and Alexandridis, A. (2011). Modeling and forecasting cumulative average temperature and heating degree day indices for weather derivative pricing. *Neural Computing and Applications* **20**(6), 787–801 (<https://doi.org/10.1007/s00521-010-0494-1>).